Molecular structure and vibrational assignments of L-tyrosine: a detailed experimental and density functional theoretical study

M.Thenmozhi[a,b], R.Mathammal[a] and C. Sekar[c,*]

[a]Department of Physics, Sri Sarada College, Salem - 636 016, TN, India.

[b]Department of Physics, Periyar University, Salem - 636 011, TN, India.

[c]Department of Bioelectronics and Biosensors, Alagappa University, Karaikudi-630 003, TN, India.

ABSTRACT

L–tyrosine ($C_9H_{11}NO_3$) is one of the 20 naturally occurring amino acids. L- tyrosine has been crystallized in silica gel by double diffusion technique which had rosette like shape. Crystal structure and spectral properties are analyzed using powder X-ray diffraction (XRD), fourier transform infrared spectroscopy (FTIR) and UV-Vis transmittance studies. Optical band gap energy of L –tyrosine crystallite is estimated as 4.28 eV. In this study, the structural properties of L-tyrosine ($C_9 H_{11} NO_3$) have been studied using density functional theory (DFT) employing B3LYP exchange correlation. The geometry of the molecule was fully optimized at B3LYP/ 6-311G (d,p) level of theory. The optimized geometrical parameters obtained by DFT calculations are in good conformity with single crystal XRD data. The vibrational frequencies were calculated and fundamental vibrations were assigned based on the scaled theoretical wavenumbers. ^{1}H and ^{13}C nuclear magnetic resonance (NMR) chemical shifts of the molecule were calculated by using the gauge-invariant atomic orbital (GIAO) method. A study on the electronic properties, such as HOMO and LUMO energies were performed by using DFT approach. Finally, geometric parameters, vibrational frequencies, chemical shifts and absorption wavelengths were compared with available experimental data of the molecule. Quantum chemical parameters such as the highest occupied molecular orbital (HOMO), the lowest unoccupied molecular orbital energy (LUMO), energy gap (ΔE), dipole moment (μ), electro negativity (χ), chemical potential (Pi), global hardness (η), softness (σ) and natural atomic charges were calculated. A good correlation was found between the theoretical data and the experimental results. The thermodynamic properties of the studied compound at room temperatures were calculated.

Introduction

Urolithiasis is a relatively common condition in humans. Dietary habits are considered the prime reasons for urolithiasis. During the last half of this century its prevalence has dramatically increased in all industrialized countries. From 3 to 20% of overall population will form at least one urinary stone during a life time of 70 years.

Crystal induced kidney disease is a frequent occurrence in human pathology. It is becoming more and more apparent that knowledge of kidney stone composition and structure appears to be the key for establishing the etiology of stone diseases. To identify pathological conditions responsible for stone formation, it is necessary to carefully examine the structure and determine both the qualitative and quantitative crystalline composition of urinary stones.

Proteins are the basic constituents of all living organisms and composed of organic molecules called amino acids which are joined covalently by peptide bonds. The building blocks of proteins are the 20 naturally occurring amino acids. These relatively simple molecules are interesting molecules themselves and much more work has been done both experimentally and theoretically in trying to understand these molecules. As building blocks of proteins, amino acids are indispensible agents of biological functions. Due to their important biological

function, amino acids have been a subject of spectroscopic studies. All α -amino acids except glycine have the same basic design i.e an amino group, a carbonyl group, and a side chain or R group, all bonded to the central carbon atom. The side chains of the 20 amino acids vary in size, shape, charge, hydrogen bonding capacity and chemical reactivity. In the main part of the -amino acid skeleton, three internal rotational degrees of freedom exist i.e rotation about the N-C, C-C and C-O bond.

Tyrosine is one of the three aromatic amino acids. Its side chain consists of a CH_2 group bonded in para position on a phenol ring. Despite its biological importance, detailed data on the conformational behaviour and spectroscopic data of neutral isolated tyrosine are not found much in literature. Matrix-isolation FTIR spectroscopic study and theoretical calculations of the vibrational properties of tyrosine were carried out by Guido Maes et al [1]. In our former report of research we have demonstrated the influence of sodium fluoride on the crystallization and spectral properties of L-tyrosine [2].

Apart from the chemical and biochemical interests of L-tyrosine, the structural and vibrational studies are of pharmacological importance because this molecule acts as a precursor of several neurotransmitters. A deficiency in the neurotransmitter synthesis can lead to physical and mental burnout and fatigue as well as Dementia, Phynylketonuria, and

depression. L- tyrosine is involved in the synthesis of melanin the dark pigment which protects against the harmful effects of ultra-violet light.

L-tyrosine is found in many protein containing foods such as meats, dairy products, fish, wheat and oats. They are products of protein metabolism and appear in urine of people with tissue degeneration or necrosis, and are present when urine is acid. L-tyrosine crystals are colorless to yellowish, brown needle shaped and have fine silky appearance. The needles may be single or arranged in sheaves or rosettes. L-tyrosine crystals usually appear in urinary sediment together with leucine crystals. Though these type of amino acids rarely occur in urinary crystals, their *in vitro* growth studies will be helpful in understanding the growth conditions of such urinary stones.

The advent of Kohn-sham density functional theory (DFT) [3, 4] in conjunction with rapid advances in computer technology has enabled accurate first principle calculations of various compounds. DFT calculations have contributed to the development of a better understanding of the fundamental properties of molecules and materials [5]. Some studies have shown that L-tyrosine acted as a good corrosion inhibitor which is known by donar-acceptor formalism. The author carried out DFT calculations with the combined Becke's three-parameter exchange functional in combination with the Lee, Yang and Parr correlation functional (B3LYP). The geometric structure, vibrational frequencies, ^1H and ^{13}C NMR chemical shifts, HOMO-LUMO energies, electric dipole moment (μ) of L-tyrosine were studied. In the present study, we have investigated the crystallization of L- tyrosine in silica gel under laboratory conditions. Spectral and non linear optical (NLO) properties of L-tyrosine are studied. Ab initio density functional theory (DFT) calculations have been performed to support our wave number assignments. On the basis of vibrational analyses, the thermodynamic properties of L-tyrosine at room temperatures have been calculated. The calculated quantum chemical parameters are E_{HOMO}, E_{LUMO}, ΔE, μ, χ, Pi, η, and σ those parameters that give valuable information about the electronic band gaps and reactive behavior.

Experimental

Sodium metasilicate (Na_2SiO_3. 9 H_2O) was used for preparing the gel and glacial acetic acid was used for adjusting the pH value. Dilute hydrochloric acid was used as the solvent for tyrosine. All the reagents used in this experiment are of analar grade. Crystallizations were conducted in the gel densities between 1.03 to 1.06 and for the pH values from 5.8 to 6.25. Optimum values of gel density and pH for the crystallization was found to be 1.06 gm/cc and 6 respectively. L- tyrosine was placed over the set gel through one of the limbs of the U tube and 0.2 M sodium hydroxide was added to the other limb. Tiny crystallites appeared at the interface between gel and L- tyrosine solution after about 15 days.

Powder X-ray diffraction pattern was recorded on Philips PW1729 diffractometer using CuKα radiation within the 2θ range of 10 to 80˚. FTIR spectra of the grown crystals were recorded using Perkin Elmer Spectrum RX1 detector and KBr beam splitter. UV - Visible spectrum was recorded on a PerkinElmer Lambda 25 spectrometer in transmission mode. Second harmonic generation efficiency of the samples was determined by Kurtz powder method. A Q switched Nd:YAG laser beam of wavelength 1064nm was used with an input energy of 1.35MJ/pulse and pulse width of 8ns, the repetition rate being 10Hz. The SHG radiations of 532 nm (green light) emitted were collected by a photo multiplier tube (PMT- Philips

photonics model 8563) and the optical signal incident on the PMT was converted into voltage output at the Cathode-Ray Oscilloscope (CRO) (Tektronix –TDS 3052B).The Raman spectral data for the title compound is taken from the literature and used for assigning the vibrational frequency, because Raman and IR spectroscopy are complimentary.

Computational details

As a first step, the most optimized structural parameters, energy and vibrational frequencies of the molecule have been calculated by using B3[6] exchange functional combined with the LYP [7] correlation functional resulting in the B3LYP density functional method at 6.311G (d,p) basis set. All the computations were performed using Guassian03W program [8] and Gauss-view molecular visualization program package on the personal computer [9]. Second, a comparison is made between the theoretically calculated frequencies and experimentally measured frequencies. In this investigation it was observed that the calculated frequencies were slightly greater than the fundamental frequencies. To improve the agreement, the frequencies are usually scaled by 0.9614 [10]. The observed disagreement between theory and experiment could be a consequence of the anharmonicity and of the general tendency to the quantum chemical methods to overestimate the force constants at the exact equilibrium geometry.

For NMR calculations, the title molecule was firstly optimized and after optimization, ^1H and ^{13}C chemical shifts (δH and δC) were calculated using the GIAO method in L-tyrosine at B3LYP method with 6-311G (d,p) basis set . The quantum chemical parameters χ, Pi and η were calculated. The obtained values of χ, and η were used to calculate the fraction of electrons transferred. The concepts of these parameters are related to each other [11-14]where:

Pi=-χ where, χ= (I+A)/2

Pi= (E_{HOMO}+E_{LUMO})/2

η= (E_{LUMO}-E_{HOMO})/2 η= (I-A)/2

Where I and A are the ionization potential and electron affinity of any chemical system, atom, ion, molecule or radical. The usefulness of χ and η lies in their ability to help predict chemical behavior. The value of η for different systems does correlate with chemical hardness and softness defined empirically.

The inverse of the global hardness is designated as the softness, σ as follows:

σ=1/η

The obtained values of χ, and η were used to calculate the fraction of electrons transferred.

Calculations of the tile compound are carried out with Gaussian 03W software program [11] using B3LYP/6-311 G(d,p) basis sets and Gauss view visualization program. To predict the molecular structure and vibrational wavenumber, calculations are carried out with using B3LYP method. Molecular structure was fully optimized by Berny's optimization algorithm using redundant internal coordinates. Harmonic vibrational wavenumbers are calculated using analytic second derivatives to confirm the convergence to minima on the potential surface. At the optimized structure Fig 3 of the title compound, no imaginary wavenumber modes are obtained, proving that a true minima on the potential surface is found. The DFT hybrid B3LYP functional tends to overestimate the fundamental modes; therefore, scaling factors have to be used for obtaining a considerably better agreement with the experimental data. The recommended scaling factor for B3LYP/6.311 **G(d,p) basis set is 0.967[13].

Results and Discussion

Crystal Growth

L-tyrosine crystallites have been successfully grown in sodium metasilicate gel. Tiny crystallites of L-tyrosine could be seen only after 15 days from the initiation of growth. Initially crystals were found to grow from the gel-solution interface into the supernatant solution and a few days later, growth started inside the gel medium also (against and towards gravity). In the supernatant solution needle shaped crystallites arranged in the form of sheaves or rosettes with fine silky appearance, whereas inside the gel medium, bunched, lengthy needles were observed. Only one rosette type of crystallites was observed in one tube .Generally the crystallites were colourless and transparent [2].

Characterisation

Powder X –ray diffraction pattern of L-tyrosine studies confirmed that L- tyrosine crystallizes in orthorhombic structure with space group $P2_12_12_1$ and the calculated lattice parameters are

a = 6.945Å, b = 21.19 Å and c = 5.858 Å which are in good agreement with JCPDS No.39-1840.

The band gap energy value E_g of the   grown crystallites have been estimated as 4.28 eV by UV-Visible transmittance studies.

FTIR analyses

FTIR spectra of L-tyrosine was recorded at room temperature in the frequency range 400 to 4000 cm^{-1} (Fig. 1) In the FTIR spectrum, the broad band lying between 3776 cm^{-1} and 2596 cm $^{-1}$are due to the absorption of the superimposed O-H, C-H and N^+H_3 stretching vibrations [15]. The strong band identified at 3776 cm^{-1} confirms the O-H stretching. The stretching vibrations of N^+H_3 result in two bands one near 3535 and other near 3211 cm^{-1} in the present study. The anti symmetric CH stretching vibrations are reported to occur in the region 3100 -3000 cm^{-1} while the symmetric stretching occurs between 3000 -2900 $cm^{-1.}$ CH_2 antisymmetric and symmetric stretching vibrations have been identified at 2934 & 2749 cm^{-1} respectively. N^+H_3 deformation bands are observed at 1515 cm^{-1} and torsional oscillation band observed at 526 cm^{-1} [16]. The strong band observed at 1607 cm^{-1} is assigned to N^+H_3 asymmetric bending vibrations.
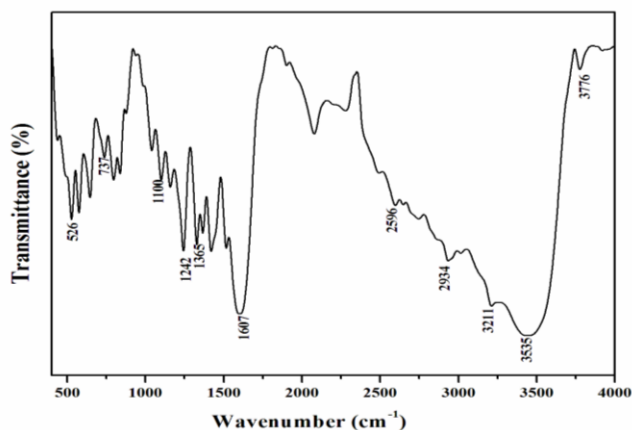
Fig 1. FTIR Spectrum of L-tyrosine

The presence of COO⁻ and N^+H_3 indicates the molecule exist in Zwitterionic form in the grown crystal [17]. The peak at 1365 cm^{-1} is assigned as CH_2 wagging. The vibrational peak at 1242 cm^{-1} is attributed to symmetric stretching of C – O. A strong band at 574 cm^{-1}, which is due to C –C – N group deformation vibration is observed for amino acids. Thus the presence of all the functional groups of L-tyrosine is confirmed by FTIR analysis.

Theoretical study

Molecular geometry

L-tyrosine is one of the aromatic amino acids with three types of donor site: namely the oxygen and the nitrogen atom of the carboxylic acid group, and the amino group [18].   The structure of the molecule with numbering scheme for the atoms is presented in Fig. 2. The global minimum energy corresponding to the optimized structure of L-tyrosine obtained by DFT calculations is -650.20740780 Hartees. The most optimized structural parameters of L-tyrosine calculated by DFT/B3LYP level with 6-311G (d,p) basis set are presented in Table 1.

The experimental and calculated geometric parameters agree well with almost all values.   In tyrosine, the optimized bond lengths of C-C in phenyl ring falls in the range from 1.390Å to 1.400Å and the optimized C5-C13 bond length is 1.5111Å. The optimized C13-C16, C-N and C=O bond lengths are 1.5569Å, 1.4554Å and 1.2062Å respectively. Molecular geometry is a sensitive indicator of intra & inter molecular interactions. The stable geometry reveals that an intramolecular hydrogen bond exists between the hydrogen atoms of amino group and oxygen atoms of the COOH group is C=O…H-NH.
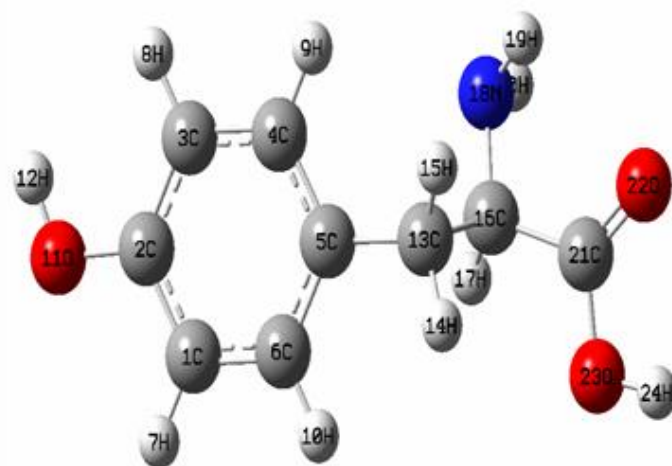
Fig 2. Optimized geometry of L-tyrosine

Vibrational assignments

The molecule L-tyrosine consists of 24 atoms. On the basis of C_1 symmetry, there are 66 fundamental vibrations.   The molecular structure has an intramolecular hydrogen bond between O-H. The normal mode of vibrations is all active in infrared and Raman spectra. A detailed vibrational description can be given by normal coordinate analysis. The observed FT-Raman and FTIR bands with their relative intensities and calculated wave numbers and assignments are given in Table 2 The experimental FTIR spectra with corresponding theoretically simulated FTIR for L tyrosine are shown in Figs. 1 and 3 respectively, where the calculated Infrared intensities and Raman intensities are plotted against the vibrational frequencies.

● **C-H Vibrations**

The broad band envelope between 2000 – 3500 cm^{-1} includes overlap of peaks due to O-H stretching of COOH, phenolic OH and NH stretching vibrations. The aromatic structure shows the presence of C-H stretching vibrations in the region 3100-3000 cm^{-1} which is the characteristic region for the identification of this group [16].

The C-H stretching vibration in the benzene derivatives arises from one non degenerate mode (3085 cm^{-1}) and two degenerate modes (3050 cm^{-1}), (2979 cm^{-1}). In this region, the bands are not appreciably affected by the nature of substituents [20].

Table 1. Optimized geometrical parameters of L-tyrosine obtained by B3LYP/6.311G (d, p) density functional theory

Atoms	Bond length (Å)[a]		Atoms	Bond angle (Å)[a]	
	Experimental[b] Value	Theoretical[a] value		Experimental[b] Value	Theoretical[a] Value
C1-C2	.	1.3941	C3-C2-C1		119.5467
C2-C3	.	1.3953	C4-C3-C2		119.7517
C3-C4	.	1.3928	C5-C4-C3		121.6942
C4-C5	1.398	1.3978	C6-C1-C2		120.0267
C6-C1	.	1.3910	H7-C1-C6		119.0455
H7-C1	.	1.0834	H8-C3-C2		119.1867
H8-C3	.	1.0865	H9-C4-C3		118.8523
H9-C4	1.085	1.0829	H10-C6-C1		119.344
H10-C6	.	1.0857	O11-C2-C1	117.9	122.7018
O11-C2	1.367	1.3710	H12-O11-C2	111.1	109.6486
H12-O11	0.989	0.9627	C13-C5-C4		120.4159
C13-C5	1.539	1.5111	H14-C13-C5		110.6493
H14-C13	1.088	1.0920	H15-C13-C5		109.1716
H15-C13	1.094	1.0952	C16-C13-C5	114.5	113.4686
C16-C13	1.539	1.5569	H17-C16-C13	110.8	110.8005
H17-C16	1.094	1.0929	N18-C16-C13	108.2	108.5811
N18-C16	1.488	1.4554	H19-N18-C16		109.756
H19-N18	1.048	1.0167	H20-N18-C16		110.938
H20-N18	1.015	1.0143	C21-C16-C13	111.1	108.9558
C21-C16	1.529	1.5295	O22-C21-C16	126.4	125.1232
O22-C21	1.259	1.2062	O23-C21-C16	117.0	112.1212
O23-C21	1.242	1.3552	H24-O23-C21		107.5011
H24-O23		0.9697			

[a] This work,[b]Ref [19]
[a] For numbering of atoms refer Fig. 2

Here in the present investigation, the FTIR and FT-Raman bands observed at 3106 cm^{-1}, 3061 cm^{-1} and 3049 cm^{-1} have been assigned to C-H stretching vibrations. Substitution sensitive C-H in plane bending vibrations appeared in the region 1000-1520 cm^{-1}and C-H out- of- plane bending vibrational wavenumbers identified at 700 and 1000 cm^{-1} [21,22,16]. In the present study, the bands corresponding to C-H in plane bending and out- of- plane bending experimental modes are in good agreement with the calculated values.

● **C-C Vibration**

The C-C stretching frequencies are generally predicted in the region 1300-1650 cm^{-1} [20-22]. Several ring modes are affected by substitution in the aromatic ring with heavy substitution, the band tend to shift somewhat to lower wave numbers. In benzene, the C-C stretching frequencies arise from the two doubly degenerated vibrations, 1591 cm^{-1} and 1532 cm^{-1} and two non-degenerate modes 1300 cm^{-1} and 998 cm^{-1} which correspond to skeletal vibrations [21,22,16]. The phenyl ring mode manifest as very intense bands in the FTIR in the frequency range 1591-1515 cm^{-1}.

● **O-H Vibration**

In vibrational spectra, the phenyl OH stretching vibration due to intra molecular hydrogen bonding determines the position of O-H band. Usually the stretching vibration of phenolic O-H groups is predicted at 4000-2000 cm^{-1} [23-26]. In the experimental spectrum of tyrosine showed a very strong absorption band is observed at 3776 cm^{-1}. In the theoretical study, an intense and sharp band is observed at 3688 cm^{-1} which can be assigned without any doubt to the υ O-H mode.

● **Methylene group vibrations**

For tyrosine the aliphatic symmetric CH_2 stretching vibration is appeared at 2749 cm^{-1} and asymmetric CH_2 stretching vibrations are observed at 2863 cm^{-1} and 2934 cm^{-1}. The various bending CH_2 vibrations are also found to be in excellent agreement with calculated data.

● **NH₂ Group Vibration**

Free amino acids have NH_3^+ stretching and deformation vibration. In the solid phase a broad absorption band is observed in the region 3390-3260 cm^{-1}. The position of the absorption depends upon degree of hydrogen bonding. The NH_2 group present in the acid is converted into $-NH_3^+$ ion during the formation of the salt. N-H and O-H groups get superimposed as they possess some common properties since N atom is less electro negative than oxygen atom, the N-H---N hydrogen bonds are weaker as compared to O-H-O bonds. Hence frequency shifts due to hydrogen bonding in amines are smaller. The asymmetrical amino stretching vibrations are predicted at 3360-3320 cm^{-1}. In the experimental study, tyrosine symmetric stretching N-H vibrations are identified at 3535 and 3211 cm^{-1}. The experimental values are in good agreement with theoretical values identified [16].

Carboxylic absorption

The carboxylic group (-COOH) is the easiest functional group to detect by infrared spectroscopy. Since this group can be considered as being formed from C=O and O-H units [27-28]. In tyrosine O-H stretching vibration observed at 3207 cm^{-1} experimentally. The O-H in plane bending vibration is observed in the region 1440-1260 cm[-1][29]. In the present study, the experimental value of in plane bending vibrations of hydroxyl group is 1318 cm^{-1}. The appearance of strong bands in the FTIR and weak bands in the Raman spectra around 1750 cm^{-1} -1650 cm^{-1} in aromatic compounds shows the presence of carbonyl group and is due to the C = O stretching motion. The wavenumber of the stretch due to carbonyl group mainly depends on the bond strength which depends upon inductive, conjugative and steric effects. Conjugation of carbonyl double bonds or aromatic rings shift the band position towards the lower wavenumbers by about 30 cm^{-1} · owing to a redistribution of electrons which weakens the C=O bonds. In the present study, the experimental frequency observed at 1686 cm^{-1} is

undoubtedly due to υ C=O. The theoretical predictions approach the experimental findings quite well.
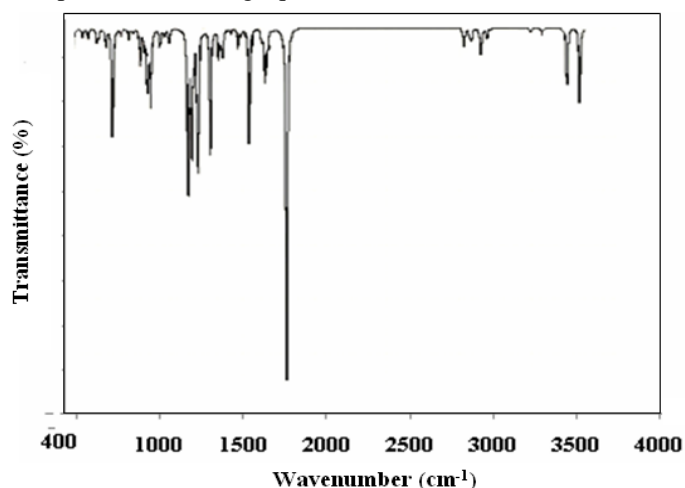
Fig 3. Theoretical IR spectrum of L-tyrosine with B3LYP/6-311G(d,p)

HOMO- LUMO analysis

The Frontier molecular orbital plays an important role in the electric and optical properties as well as in the UV-visible spectra and chemical reaction. The electronic absorption corresponds to the transition from the ground to the first excited state and is mainly described by one electron excitation from the highest occupied molecular orbital (HOMO) to the lowest unoccupied molecular orbital (LUMO). The HOMO-LUMO energy of L-tyrosine was calculated at DFT B3LYP/6-311G(d,p) levels shown in the Table 3 which reveals that the energy gap reflects the chemical activity of the molecule. The LUMO as an electron acceptor represents the ability to donate an electron. Moreover, a lower HOMO-LUMO energy gap explains the fact that eventual charge transfer interaction is taking place within the molecule [31]. Since molecular orbital (MO) theory is by far the most widely used by chemists, it is important to place χ and η in a MO framework. The conjugated molecules are characterized by a highest occupied molecular orbital-lowest unoccupied molecular orbital (HUMO-0LUMO) separation, which is the result of a significant degree of intermolecular charge transfer (ICT) from the end-capping electron-donor to the efficient electron acceptor group through π conjugated path.
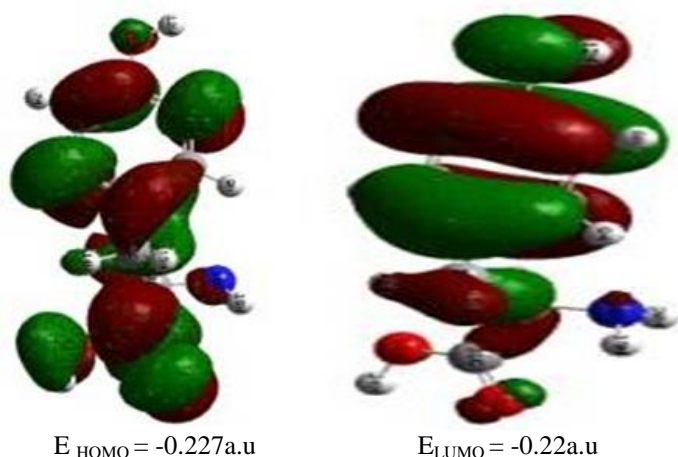
$E_{HOMO} = -0.227$a.u $E_{LUMO} = -0.22$a.u
Fig. 4 (a) HOMO and (b) LUMO plot of Frontier molecular orbitals for L-tyrosine

It has already been shown that the MO theory of the chemical bond contains the values of χ and η for the bonding

fragments. Within the validity of Koopmans' theorem [32], the frontier orbital energies are given by

$-E_{HOMO} = I$ and $-E_{LUMO} = A$.

Negative χ is equal to the electronic chemical potential μ [31,33]. The energy gap between the HOMO and LUMO is equal to 2η. Hard molecules have a large HOMO-LUMO gap and soft molecules have a small energy HOMO-LUMO gap (Fig. 4.3).

NMR spectral analysis

The NMR serves as a great resources in determining the structure of an organic compound by revealing the hydrogen and carbon skeleton. The calculated values for ^{13}C and ^{1}H NMR are shown in Table 4. The studied molecule shows six different carbon atoms which is consistent with the structure on the basis of molecular symmetry. [1]H and ^{13}C chemical shift values (with respect to TMS) have been calculated for the optimized structures of the title compound. The chemical shift values of C21, C13, and C16 have been observed at 183.482 ppm (C=O), 44.8661ppm (C-H) and 60.7143 ppm respectively. In the present work, ^{13}C NMR chemical shifts in the ring are > 100 ppm, as they would be expected. Due to the electronegative property of oxygen atom, the chemical shift value of C21 and C2 has bigger value than the other carbons. The chemical shift of carboxyl carbon is observed in the down field due to partial ionic nature of the carboxyl group because chemical shifts used as an aid in the identification of reactive organic as well as ionic species. The formation of hydrogen bonds leads to a significant downfield shift of the isotropic chemical shifts. If hydrogen-bond formation involves amino protons and the carbonyl group, the direction of the electron density shift from the N-H to the carbonyl group results in a decreased magnetic shielding for the amino proton and hence results in a shift to lower field of its proton signal. The high electronegative property of N atom polarizes the electron distribution in its bond to the adjacent carbon atom.

NBO analysis

NBO analysis clearly manifests the evidence of the intra molecular charge transfer and intra molecular bonding. The atomic and natural atomic charges of L-tyrosine are given in Tables 5 and 6 respectively. The σ-electron-withdrawing character of the COOH, NH₂ atoms is demonstrated by a decrease of electron density on the C1, C2, C3 atoms. The H24, H12, C21 atoms of L-tyrosine can accommodate higher positive charge and become more acidic. Then O22 (-0.60920) and N18(-0.90209) atoms in L-tyrosine have higher negative charge because of electron withdrawing nature.

MULLIKEN atomic charges

Mulliken atomic charge calculation has an important role in calculating the lot of properties of molecular system. The charge on the nitrogen atom exhibits a substantial negative charge which is donor atom. Hydrogen atom exhibits a positive charge which is an acceptor atom.

Other Properties

Several thermodynamic properties like heat capacity, zero point energy, entropy along with the global minimum energy of L-tyrosine have been obtained by ab initio density functional methods using 6.311G (d,p) basis set calculations are presented in Table 7. The polarity of the molecule is well known to be important for physio chemical properties. The dipole moment is the most widely used quantity to describe the polarity of a molecule. Dipole moment reflects the molecular charge distribution and is given as a vector in three dimensions.

Table 2. Detailed assignment of fundamental vibrations of L-tyrosine based on SQM force field calculation

Sl.No	Observed wavenumber cm^{-1}		Calculated wavenumbers B3LYP/6-311G(d,p) force field cm^{-1}		IR Intensity	Vibrational Assignment
	FTIR[a]	Raman[b]	Unscaled	scaled		
1	3776.04	-	3836.13	3688.05	68.185	υ OH
2	3435.37	-	3747.99	3603.31	67.298	υ OH
3	3211.52	-	3574.43	3436.45	8.0349	υ$_{as}$NH$_2$
4	3203	3207	3496.03	3361.08	4.0053	υ$_s$NH$_2$
5	3106	-	3194.99	3071.66	1.9888	υCH(R)
6	-	3061	3191.89	3068.68	9.3836	υCH(R)
7	3040	-	3157.06	3035.19	8.9445	υCH(R)
8	-	-	3148.88	3027.33	22.2348	υCH(R)
9	2934	-	3084.41	2965.35	15.2627	υ$_{as}$CH$_2$
10	-	2863	3069.61	2951.12	7.0722	υ$_{as}$CH$_2$
11	2749		3031.86	2914.83	19.1413	υ$_s$CH$_2$
12	1686	-	1803.57	1733.95	342.268	υC=O
13	1607	1615	1670.89	1606.39	32.568	φNH
14	1591	-	1653.70	1589.86	50.188	υCC(R)
15	1532	-	1631.40	1568.42	15.2283	υCC(R)
16	1515	-	1543.91	1484.31	111.799	υCC(R)
17	1436	-	1488.80	1431.33	7.8607	φHCH
18	1419	-	1466.80	1410.18	19.1414	φHCC(R)
19	1377	-	1420.16	1365.34	5.406	φHCN
20	-	-	1361.65	1309.09	17.6781	φHCC
21	1365	-	1359.36	1306.88	7.2117	φHCH
22	1327	1328	1349.74	1297.65	13.6551	φCH
23	1318	-	1332.28	1280.85	30.5841	φOH
24	1242	1267	1297.61	1247.52	2.2914	φHNC
25	-	1249	1276.18	1226.91	116.23	υCO
26	1216	-	1263.33	1214.56	8.721	φCH
27	1209	-	1227.06	1179.69	0.8692	υCC(adjR)
28	1191	-	1196.88	1150.68	8.1338	φHOC(R)
29	-	1180	1188.06	1142.20	157.588	φHCC(R)
30	1158.25	-	1159.44	1114.68	30.8517	φHCH
31	1100	-	1146.01	1101.77	123.609	φHCN
32	-	-	1122.32	1078.99	151.97	φCH
33	1040.15	-	1114.09	1071.08	26.786	υNC
34	-	980	1030.40	990.626	1.3639	φCCC
35	964	967	989.756	951.550	14.7144	υCC(adjN)
36	-	935	969.038	931.633	1.1636	ωHCCC(R)
37	-	899	954.429	917.588	8.1768	ωHCCH
38	876	-	924.857	889.157	21.6181	ωCH
39	-	855	879.656	845.700	0.6455	φHCH
40	837	-	863.727	830.387	73.3097	φNH$_2$
41	808	-	844.209	811.620	42.5754	φNH$_2$
42	796	-	8340792	802.569	55.7296	ωCH
43	-	-	813.823	782.400	16.7049	υCC
44	737	-	787.844	757.430	35.3717	φCCC
45	715	-	738.409	709.906	5.5244	ωCH$_2$
46	645	-	709.206	681.830	12.0056	τCCCC
47	613	-	6570213	631.844	3.218	φCCO(R)
48	593	-	653.421	628.198	6.0717	φCCN(adjO)
49	574	-	597.020	573.970	124.949	τHOCC(adjN)
50	526	-	550.288	529.046	18.9093	ωCCCC(R)
51	499	-	500.920	481.580	10.1296	ωCCCC(R)
52	-	457	486.899	468.104	14.2375	φCCC(R)
53	437	433	428.191	411.660	10.7429	φCCO(R)
54	-	-	420.212	403.990	2.001	τCCCC(R)
55	-	386	389.830	374.780	9.4771	φCCN(adjR)
56	-	338	357.284	343.492	1.7585	φCCN(adjR)
57	-	-	310.820	298.820	102.007	τHOCC(R)
58	-	-	298.772	287.239	17.9415	τHNCC(adjR)
59	-	196	269.022	258.630	0.8899	φCCC(adjR)
60	-	185	215.725	207.390	27.7321	φCCO(adjN)
61	-	178	185.734	178.560	0.4199	τCCCO(R)
62	-	145	176.408	169.59	1.1402	φCCC(adjO)
63	-	64	69.4329	66.752	1.0251	τCCCC
64	-	58	58.4174	56.162	0.8795	ωCCCN
65	-	36	44.2581	42.549	1.1916	τCCCO
66	-	28	32.1479	30.906	1.2058	τ$_{ring}$

υ : stretching; τ: torsion; s: symmetry; as: antisymmetry; R: Ring; φ: bending; adj: adjacent ; ω : wagging;
[a] IR-present work ; [b] Reference from [30].

Table 3. Calculated quantum chemical parameters of the L-tyrosine

Parameters	Values
E_{HOMO}	-0.227
E_{LUMO}	-0.022
ΔE	0.205
X	0.1025
H	0.1025
Σ	9.756

Table 4. Calculated ^{13}C NMR and ^{1}H NMR Chemical shifts (ppm) of L-tyrosine

Carbon [a]	Chemical shifts	Proton [a]	Chemical shifts
C_1	118.304	H_7	6.95815
C_2	162.277	H_8	6.41496
C_3	115.625	H_9	7.59929
C_4	137.723	H_{10}	7.19858
C_5	136.83	H_{12}	3.60997
C_6	134.821	H_{14}	2.69279
C_{13}	44.8661	H_{15}	2.22084
C_{16}	60.7143	H_{17}	3.04007
C_{21}	183.482	H_{19}	1.25913
		H_{20}	0.564559
		H_{24}	5.64915

For numbering of atoms refer Fig. 2

Table 5. Atomic charges for optimized geometry of L-tyrosine obtained by B3LYP/ 6.311G(d,p) density functional calculations

Atoms [a]	Mulliken	Atoms [a]	Mulliken
C_1	0.230673	C_{13}	-0.657504
C_2	-0.451254	H_{14}	0.154699
C_3	0.039373	H_{15}	0.165144
C_4	-0.616407	C_{16}	-0.269370
C_5	1.680228	H_{17}	0.188749
C_6	-0.698512	N_{18}	-0.375926
H_7	0.127560	H_{19}	0.234712
H_8	0.103814	H_{20}	0.228398
H_9	0.124584	C_{21}	-0.118040
H_{10}	0.115195	O_{22}	-0.292007
O_{11}	-0.261962	O_{23}	-0.167720
H_{12}	0.246252	H_{24}	0.269320

For [a] numbering of atoms refer Fig. 2

Table 6. Natural atomic charges for L-tyrosine: Calculations performed at the B3LYP/6.311G(d,p) level of theory

Atoms[a]	Natural atomic charges	Atoms[a]	Natural atomic charges
C_1	-0.31655	C_{13}	-0.47324
C_2	-0.32412	H_{14}	0.24788
C_3	-0.28863	H_{15}	0.25204
C_4	-0.21641	C_{16}	-0.15770
C_5	-0.07233	H_{17}	0.26354
C_6	-0.20155	N_{18}	-0.90209
H_7	0.23080	H_{19}	0.39127
H_8	0.24884	H_{20}	0.38912
H_9	0.23629	C_{21}	0.81777
H_{10}	0.25321	O_{22}	-0.60920
O_{11}	-0.69353	O_{23}	-0.71689
H_{12}	0.49013	H_{24}	0.50308

For numbering of atoms[a] refer Fig. 2

Table 7. Theoretically computed energies (a.u.), Zero-point vibrational energies (kcal mol^{-1}), Rotational constants (GHz), Entropies (cal mol^{-1} K^{-1}), Nuclear repulsion energy (hartrees) and Dipole moment (Debye) for L-tyrosine

Parameters	Values
Zero-point energy	120.99819
Rotational constants	2.2746, 0.3418, 0.38
-V/T	2.009
Entropy	
Total	112.163
Translational	41.488
Rotational	31.568
Vibrational	39.107
Dipole moment	0.678
Nuclear repulsion energy	758.533

Therefore, it can be used as descriptor to depict the charge movement across the molecule. Direction of the dipole moment vector in a molecule depends on the centers of positive and negative charges. Dipole moments are strictly determined for neutral molecules. For charged systems, its value depends on the choice of origin and molecular orientation. Scale factors have been recommended [33] for an accurate prediction in determining the zero-point vibration energy (ZPVE), and the entropy (S_{vib}). The variation in the ZPVE seems to be insignificant.

Conclusions

L–tyrosine ($C_9H_{11}NO_3$) crystallites have been grown in silica gel by double diffusion technique and the morphology has rosette like shape.. FTIR spectra confirm the presence of all the functional groups and Zwitter ionic form. Optical studies of the grown crystals show the band gap energy of L-tyrosine crystal as 4.28 eV. The structural properties of L-tyrosine were studied using density functional theory (DFT) employing B3LYP exchange correlation. The geometry of the molecule was fully optimized at B3LYP/6-311G(d,p) level of theory. The vibrational frequencies were calculated and fundamental vibrations were assigned based on the scaled theoretical wave numbers. The computed geometrical parameters are in good agreement with the observed X-ray data. [1]H and ^{13}C nuclear magnetic resonance (NMR) chemical shifts of the molecule were calculated by using the gauge-invariant atomic orbital (GIAO) method. A study on the electronic properties such as HOMO and LUMO energies were performed. Finally, geometric parameters, vibrational bands, chemical shifts and absorption wavelength were compared with available experimental data of the molecule. Quantum chemical parameters such as the highest occupied molecular orbital (HOMO), the lowest unoccupied molecular orbital energy (LUMO), energy gap (ΔE), dipole moment (μ), electro negativity (χ), chemical potential (Pi), global hardness (η), softness (σ) and natural atomic charges were calculated. A good correlation was found between the theoretical and the experimental results.

References

[1] R. Ramaekers, J. Pajak, M. Rospenk, G.Maes Spectrachimica Acta Part A   61 (2005) 1347-1356.
[2] M. Thenmozhi, K. Suguna, C. Sekar, Spect.chim. Acta Part A, 84 (2011) 37.
[3] P. Hohenberg, W. kohn, Inhomogeneous electron gas, Phys. Rev.136 (1964) B864-B871.
[4] W. Kohn, L.J. Sham, Self-consistent equations including exchange and correlation effects, Phys. Rev. 140 (1965) A1133-A11328.
[5] F.M. Bickelhaupt, E.J. Baerends, Reviews in Computational Chemistry, Wiley-VCH, New York, 2000. A.D.
[6] A.D.Becke, J. Chem. Phys., 98 (1993) 5648.
[7] C. Lee, W. Yang, R.G. Parr, Phys. Rev., B, 37 (1988) 785.
[8] M. J. Frisch, G. W. Trucks, H. B. Schlegel, G. E. Scuseria, M. A. Robb, J. R. Cheeseman, J. A. Montgomery, Jr., T. Vreven, K. N. Kudin, J. C. Burant, J. M. Millam, S. S. Iyengar, J. Tomasi, V. Barone, B. Mennucci, M. Cossi, G. Scalmani, N. Rega, G. A. Petersson, H. Nakatsuji, M. Hada, M. Ehara, K. Toyota, R. Fukuda, J. Hasegawa, M. Ishida, T. Nakajima, Y. Honda, O. Kitao, H. Nakai, M. Klene, X. Li, J. E. Knox, H. P. Hratchian, J. B. Cross, C. Adamo, J. Jaramillo, R. Gomperts, R. E. Stratmann, O. Yazyev, A. J. Austin, R. Cammi, C. Pomelli, J. W. Ochterski, P. Y. Ayala, K. Morokuma, G. A. Voth, P. Salvador, J. J. Dannenberg, V. G. Zakrzewski, S. Dapprich, A.

D. Daniels, M. C. Strain, O. Farkas, D. K. Malick, A. D. Rabuck, K. Raghavachari, . B. Foresman, J. V. Ortiz,Q. Cui, A. G. Baboul, S. Clifford, J. Cioslowski, B. B. Stefanov, G. Liu, A. Liashenko, P. Piskorz, I. Komaromi, R. L. Martin, D. J. Fox, T. Keith, M. A. Al-Laham, C. Y. Peng, A. Nanayakkara, M. Challacombe, P. M. W. Gill, B. Johnson, W. Chen, M. W. Wong, C. Gonzalez, and J. A. Pople, Gaussian03, Revision E.01, Gaussian Inc., Walllingford, CT, (2004).
[9] A. Frisch, A. B. Nielsen, A. J. Holder, Gaussview Users Manual, Guassian Inc., Pittsburgh, (2007).
[10] W. A. Guillory, Introduction to Molecular Structure and Spectroscopy, Allyn and Bacon Inc., Boston, (1977).
[11] R. G. Parr, D.Al. Donnelly, M. Levy, M. Palke, J. Chem. Phys. 68 (1978) 380.
[12] R.G. Parr, R.G. Pearson, J. Am. Chem. Soc, 105 (1983) 7512.
[13] R.G. Pearson, Inorg, Chem. 27 (1988) 734.
[14] P. Geerlings, F. De proft, W. Langenaeker, Chem. Rev. 103 (2003) 1793.
[15] B. N. Moolya, S. M. Dharmaprakash, J. cryst. growth 290 (2006) 498.
[16] G.Socretes, Infrared and Raman Characteristic Group Frequencies, John-Wiley, Chichester (1980).
[17] Nakamato, Infrared and Raman spectra of inorganic and co-ordination compounds, 3 rd edition, John wiley interscience Newyork.
[18] E. F. H. Brittain, W. O. George, C. H. J. Wells, Introduction to Molecular Spectroscopy – Theory and Experiment, Academic Press, London, (1970).
[19] M. N. Frey, T. K. Koetzle, M. S. Lehmann, W. C. Hamilton, J. Chem. Phys, 5816 (1973) 2547.
[20] N. P. G. Roeges. A Guide to Complete Intepretion of infrared Spectra of Organic Structures, Wiley, Newyork, (1994).
[21] L. J. Bellamy, The Infrared Spectra of Complex Molecules Chapman and Hall Ltd., London, (1975).
[22] G. Varsanyi, Assignments for Vibrational spectra of Sevenhundered Benzene Derivatives, Vols, 1 and 2, Adam Hilger, (1974).
[23] S. A. Brandán, F. Marquez Lopez, M. Montejo, J. J. Lopez Gonzalez, A. Ben Altabef, Spectrochim. Acta Part A, 75 (2010) 1422.
[24] J. Antony, G. Von Helden, G. Meijer, B. Schmidt, J. Chem. Phys. 123 (2005) 14305.
[25] M. Urbanová, V. Setnicka, F. J. Devlin, P. J. Stephens, J. Am. Chem. Soc., 127 (2005) 6700.
[26] G. Keresztury, F. Billes, M. Kubinyi, T. Sundius, J. Phys. Chem., A 102 (1998) 1371.
[27] Y. R. Sharma, Elementary organic spectroscopy - Principles and chemical applications, S. Chand and Co, New Delhi, (2010).
[28] Jag Mohan, Organic spectroscopy Principle and Applications, Narosa Publishing House, NewDelhi, (2011).
[29] D. N. Sathyanarayanan, Vibrational Spectroscopy Theory and Application, New Age International publishers, New Delhi, (1996).
[30] C. D. Contreras, A. E. Ledesma, H. E. Lanus, J. Zinczuk, S. A Brandan, Vibrational Spectroscopy 57 (2011) 108.
[31] M. Arivazhagan, S. Jeyavijayan Spectrochimica Acta Part A, 79 (2011) 376.
[32] T. Koopmans, Physica 1 (1934) 104.
[33] P. Mani, H. Umamaheswari, B. Dominic. Joshua, N. Sundaraganesan, Journal of Molecular Structure, THEOCHEM, 863 (2008) 44.